Aeroacoustics of a Parallel Blade-Vortex Interaction using Indicial Method

Rajneesh Singh
Research Assistant

James D. Baeder
Associate Professor

Alfred Gessow Rotorcraft Center
Department of Aerospace Engineering
University of Maryland at College Park, MD 20742

Abstract

Aeroacoustics of a Parallel Blade-Vortex Interaction (BVI) is investigated using the indicial method. A new generalized gust function is developed as a function of the gust ratio and Mach number for an airfoil penetrating a moving gust. BVI occurring on the advancing blade is modeled as an interaction of a prescribed isolated line vortex of known strength with a rotor blade in forward flight. The indicial method with a general gust function (along with 3-D coupling) is applied to determine the linear unsteady aerodynamic lift time history. An Euler method is used to calculate the nonlinear aerodynamics. Acoustic pressure signals at far-field observer locations are calculated using classical surface monopoles and dipoles for the linear acoustic propagation. The accuracy of the indicial method is demonstrated by comparing with the results obtained using the Euler method to predict unsteady aerodynamic lift. The far-field noise is calculated for a range of vortex speed ratios; it is shown that the vortex convection speed significantly influences the noise magnitude. Furthermore, it is shown that the vortex convection effects can be accurately modeled with linear unsteady aerodynamics by using the newly developed general gust function.

Introduction

Blade-vortex interactions (BVI) are one of the most important sources of unsteady loading and noise for a helicopter. Such interactions occur when the tip vortices shed by preceding blades induce impulsive changes in the downwash on successive blades. The resulting rapid changes in the blade loading produce sharp noise pulses. Although BVI can occur at various locations around the rotor azimuth, the strongest interaction noise usually occurs on the advancing side when the blade is at an azimuthal angle of 70 to 80 degrees. The reasons are twofold: (1) at this point the interaction angle between the vortex and the blade is nearly parallel and the unsteady loading along the span of the blade is in phase; and (2) the Doppler amplification factor is greater for the larger local Mach numbers on the advancing side. Such an interaction is called a parallel blade vortex interaction.

In forward flight the forward motion of the rotor system results in the downstream convection of the tip vortices that initially follow an epicycloidal pattern. As the tip vortices convect downstream their interaction with the rotor system, as well as mutual self-interactions, results in velocity perturbations which cause the tip vortices to move at velocities different from the freestream. The gust speed ratio is a parameter which can be used to represent the convection speed of the vortex through the freestream flow. The speed ratio, λ, for a sharp edged gust is defined as:

$$\lambda = V/(V + V_g) \tag{1}$$

where V is the freestream velocity and V_g is the velocity of gust with respect to the freestream. Thus $\lambda < 1$ represents a faster moving gust with $\lambda = 0$ corresponding to an indicial change in the angle of attack. Similarly $\lambda > 1$ represents a slower moving gust. Typically λ varies from 0.9 to 1.3 for a rotor in forward flight.

The convection velocity of the vortex influences the acoustics of BVI in two ways. One, the time history of the unsteady gust field induced by the vortex at a given point on the blade changes with the vortex convection velocity. The relative velocity between the blade and the vortex determines the time period of the interaction. For a faster moving vortex, the interaction occurs over a shorter interval

of time, resulting in a more rapid change in the unsteady loads. This effect can be accounted for by knowing the location of the vortex relative to the blade.

Secondly, the aerodynamic response of the airfoil section changes. For an airfoil penetrating a moving gust the lift consists of two components. The circulatory component is associated with the instantaneous bound circulation on the airfoil. The circulatory lift starts from zero at the instant airfoil penetrates the gust front and asymptotically reaches the steady state magnitude corresponding to the angle of attack induced by the gust. Another contribution to the total lift comes from the impulsive change in the boundary condition on the airfoil element entering the gust. A step change in the boundary condition results in a compression wave on the one surface and an expansion wave on the other surface. This pressure differential results in lift on the airfoil which decays rapidly within a few chord distances of airfoil travel. This non-circulatory lift is fairly small for a stationary gust but its contribution increases as the gust speed ratio decreases. In the limiting case of an infinitely fast moving gust (a step change in angle of attack), the total lift at initial times is dominantly non-circulatory. Currently, aerodynamic comprehensive codes neglect the changed aerodynamic response, utilizing the stationary gust response for all gusts (i.e. the non-circulatory lift is neglected).

A good review of the general indicial concept is given by Lomax[1] and Tobak and Schiff[2] with applications in the field of rotary wing aerodynamics by Beddoes[3] and Leishman[4]. In brief, the indicial method to determine the unsteady aerodynamic response to an arbitrary input consists of using Duhamel superposition of indicial responses of that input. The indicial response is the response of the aerodynamic flowfield to a step change in a set of defined boundary conditions, such as a step change in angle of attack, pitch rate, or a penetrating gust field. For example, the gust indicial response is the aerodynamic response of an airfoil penetrating a gust of unit magnitude. Knowledge of the gust indicial response is sufficient to determine the unsteady loads for an airfoil subject to an arbitrary gust field. For 3-D applications, the indicial method can be extended by including a method to account for 3-D coupling (due to trailed vorticity) effects.

Figure 1 shows the aerodynamic response of an airfoil in a freestream Mach number of 0.5 penetrating a moving gust at various gust speed ratios (as determined from 2-D Euler calculations by Singh and Baeder[5]). The lift time history is plotted against time, non-dimensionalized by semichord and the free stream Mach number. It can be observed from the figure that the gradient of the lift time history increases with the gust convection speed. The accurate prediction of the acoustics requires the initial slope to be represented accurately, as will be discussed in the next section. The dependence of the gust response on the gust speed ratio then manifests itself in the change in the coefficients of the gust function.

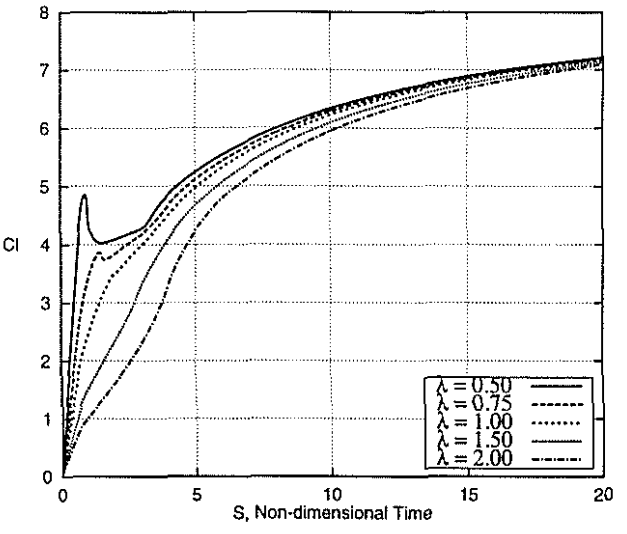

Figure 1: Lift time history for various gust speed ratios for an airfoil penetrating a moving gust at freestream Mach number of 0.5 [6].

For a helicopter rotor in forward flight, both the Mach number and the gust speed ratio vary with azimuth and span. To avoid the computationally expensive process of a table lookup or interpolation it is desirable to have a representation of the gust function in the form of a function of Mach number and gust speed ratio. For practical applications, an exponential form of the gust function allows for the formulation of the Duhamel integral as a one-step recursive algorithm. Fortunately, the asymptotically exponential behavior of the indicial function is sufficiently close to the physical behavior such that a few exponential function terms can accurately approximate the indicial response. In this work such a gust function is used, which further improves the efficiency of the method. An indicial method with exponential indicial functions has been shown to be several order of magnitude faster compared to the more rigorous CFD methods to determine unsteady loads. Furthermore, the agreement with CFD is excellent if the approximate indicial functions utilized are themselves based on

CFD calculations.

The main objective of this study is to apply the indicial method with a general gust function to better simulate the effects of vortex convection. To this end, a model problem consisting of an isolated rotor blade interacting with a single line vortex of known strength is examined. The unsteady aerodynamic loading and far-field noise is calculated for various convection speeds of the vortex to examine the significance of vortex convection effects.

Figure 2 shows the sketch of the computational model. The plan view shows the rotor rotating in a counter-clockwise direction. A line vortex convects in a straight line at a fixed distance below the blade. The velocity of the vortex convection is determined by the gust speed ratio parameter. The vortex is initialized such that when the blade reaches the 90 degree azimuthal location the vortex is directly underneath the quarter-chord of the blade.

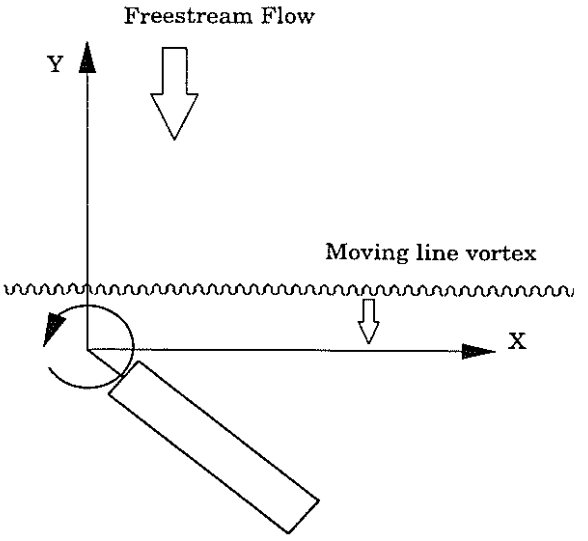

(a) Plan View

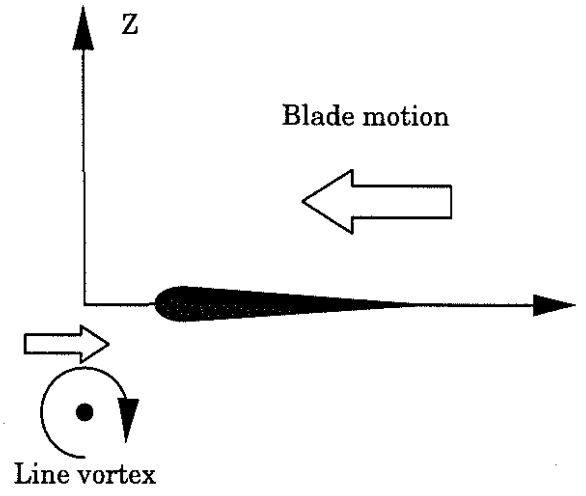

(b) Side View

Figure 2: Sketch of the computational model for the interaction of an isolated line vortex with an isolated rotor blade at 90 degree azimuthal angle.

Approach

Gust Function Development

As mentioned earlier, an exponential form of the gust response is sought for computational efficiency. In a previous study this was obtained for one Mach number[5], with the number of terms and their coefficients chosen to best approximate 2-D indicial calculations performed using a 2-D Euler solver[5], as well as satisfy exact theoretical analytical conditions at the beginning of the indicial calculations[6].

In this study a four term representation was chosen, as a three term representation was found to be inadequate to fit the gust response while a five term representation did not show any significant improvement over the four term gust function. The general gust function is parametrized for both the gust speed ratio and the Mach number. The following form of the gust function was chosen in this study to set up the optimization problem:

$$C_L(S,\lambda,M) = C_{l_\alpha}\left(1+\sum_{i=1}^{4} A_i(\lambda,M)\exp(-B_i(\lambda,M)S)\right)$$

where $A_1 ... A_4$ and $B_1 ... B_4$ are the coefficients to be determined and $C_{l_\alpha} = 2\pi/\beta$ is the lift curve slope. Of the 8 coefficients contained in the above representation, two are determined by applying the constraint at $S = 0$ on the lift magnitude and its time derivative. An analytic expression can be obtained for the gust response for a short period of time by making use of analogy between equations governing 2-D unsteady flow with 3-D steady supersonic flow. The analytic expression is then used to determine the time derivative of the lift at $S = 0$.

It is desired to associate exponential terms of the approximate gust function with the unsteady pro-

cesses taking place during the interaction. However, in this study, the remaining 6 coefficients are arbitrarily expressed as functions of M and λ. The main motivation being to use simple polynomial functions to adequately approximate the gust response over a range of parameters. Several functions were tried out to minimize the error in a least square sense to the lift time history obtained from an Euler solver. The following expressions were determined to best represent the gust response:

$$\begin{aligned} A_1 &= c_1 + c_2\lambda/(1+\lambda) \\ A_2 &= c_3 + c_4\beta \\ A_3 &= c_5 + c_6\beta^2 \\ B_1 &= c_7 \\ B_2 &= c_8\lambda + c_9\beta \\ B_3 &= c_{10} \end{aligned}$$

The constraints on C_L and its gradient at $S = 0$ determine A_4 and B_4 as:

$$\begin{aligned} A_4 &= -1 - A_1 - A_2 - A_3 \\ B_4 &= -(\frac{dC_L/dS}{C_{L_\alpha}} + A_1B_1 + A_2B_2 + A_3B_3)/A_4 \end{aligned}$$

where $\beta = \sqrt{1-M^2}$ and $dC_L/dS = 2.8/\sqrt{M\lambda^3}$. The value of the slope used for the constraint is higher than the theoretical initial value to allow for the exponential decay: thus, optimizing the slope over the short initial time period.

The coefficients $c_1 ... c_{10}$ were then obtained by simultaneously optimizing on a CFD database over the range of $M = 0.4$ to 0.65 at every 0.05 and λ ranging from 0.8 to 1.4 at the interval of every 0.1. The coefficients had the following magnitudes: $c_1 = -3.305$, $c_2 = 2.762$, $c_3 = -0.080$, $c_4 = 0.134$, $c_5 = 2.548$, $c_6 = 1.680$, $c_7 = 0.183$, $c_8 = 0.514$, $c_9 = 1.492$ and $c_{10} = 0.344$.

Aerodynamics Calculations

The problem of determining the unsteady load distribution over a rotor blade is complex because of two reasons. First, the shed vortices induce a downwash over the blade that feeds back and influences the load distribution accordingly. This effect is already implicitly contained in the 2-D indicial response functions. Second, the trailed vortices, due to the distribution of spanwise loading, reduce the loads near the blade tip region. This is not contained in the 2-D indicial response functions.

In discrete time a finite-difference approximation to the Duhamel integral results in a one-step recursive method. For the present study, an indicial method[7] with the generalized gust function is used to calculate the unsteady aerodynamic load history for the BVI. At each azimuth location of the rotor blade, the downwash induced by the isolated line vortex is calculated at the quarter chord using an algebraic core model due to Sculley and Kaufmann. The 2-D indicial response must be modified to include the 3-D effects. Rather than an empirical correction, a better method to accurately account for the 3-D effects is a Weissinger-L model. The Weissinger-L method is a limiting case of the lifting surface method with only one surface element in the chordwise direction. In this study the Weissinger-L method is used with the unsteady airloads computed at 36 radial stations along the span of the blade at time intervals of one-half a degree in azimuth. The trailing vortices in the method are tracked for an azimuthal length equal to the azimuthal extent of the grid in the CFD calculations (approximately 70 degrees of wake age) used for the non-linear aerodynamics computations. As stated earlier, the shed wake is not explicitly calculated, but rather is contained implicitly in the 2-D indicial responses. The complete airloads calculation requires less than one minute of CPU time on a DEC Alpha workstation.

The Transonic Unsteady Rotor Navier-Stokes (TURNS)[8] code is used as an Euler solver to calculate the aerodynamics of the BVI. The TURNS code is a finite-difference code to solve Navier-Stokes equations and it has been applied to a variety of helicopter aerodynamic and acoustic problems[9-11]. It uses Roe upwinding with higher order MUSCL type limiting on the right hand side for spatial accuracy. A LU-SGS implicit operator is used on the left hand side to increase stability and robustness. Unfortunately, the use of a spectral radius approximation in the implicit scheme renders the method only first order accurate in time. Therefore, in this study a second order backwards difference in time is used along with Newton type sub-iterations to restore formal second order accuracy in time. This also reduces the factorization and linearization errors associated with the scheme. In this study viscous effects are ignored and the code is only used in Euler mode. The convection of the line vortex is incorporated using the field velocity approach.[12]

CFD calculations were performed on a C-H grid topology. The grid had 169 points in the wrap-around direction with 131 points on the blade sur-

face, 49 points in the spanwise direction with 35 points on the blade surface and 43 points in the normal direction. Following the calculation of the initial quasi-steady state solution for each of the flight conditions, unsteady computations are performed for a time-step of 0.2 degree. The CFD solution was found to be insensitive to increased refinement in either space or time. One calculation required approximately 10 hours of CPU time on a DEC Alpha workstation.

Acoustics Calculations

The WOPWOP [13] code is used to calculate the far-field acoustic pressure. This code is based on Lighthill's acoustic analogy [14] in the form of the Ffowcs Williams-Hawkings (FW-H) equation[15]. This code models the helicopter rotor acoustics relatively accurately and requires the blade surface pressure distribution and the blade motion as input. Formula 1A of Farrasat is used. This brings the time derivative inside the integral, causing the time derivatives of the source terms to be required. Furthermore, the integration to determine the pressure time history at a given observer location and time requires the solving of the retarded time equation and the subsequent interpolation of the observer sources and time derivatives of sources. The pressure distribution is specified on the top and the bottom airfoil surface for the unsteady aerodynamics calculation using CFD while it is specified on the mean surface for the indicial method using the analytical flat plate distribution. For compact acoustic sources the blade lift time history is sufficient to determine the far-field acoustics signature; however, for non-compact sources a chordwise pressure distribution over the blade surface is required. This is obtained by using the analytical pressure distribution corresponding to a flat plate in linear flow at an angle of attack. This distribution is given by:

$$C_p(x) = \frac{2C_l}{\pi}\sqrt{(1-x)/x}$$

where x is the distance as a fraction of the chord length from the leading edge.

Results and Discussion

As mentioned earlier, during low-speed descent, typical of terminal operations, the rotor blades may encounter the large velocity gradients generated by the trailed tip vortices. The rapidly changing induced velocity field causes large, time varying fluctuations in loading on the blade. The resulting

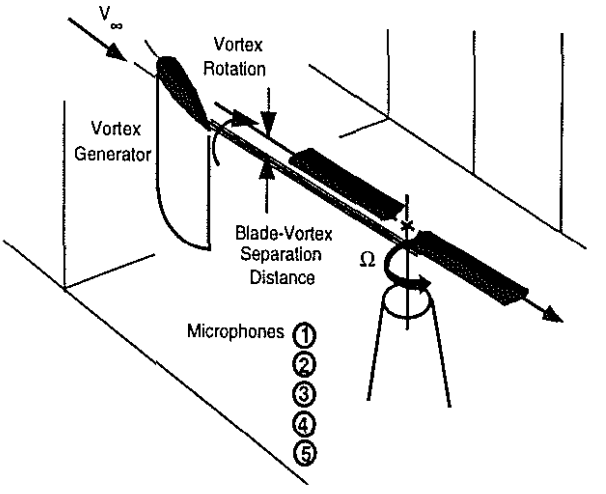

Figure 3: Sketch of the experimental setup of Kitaplioglu and Caradonna.

blade-vortex interaction noise is then dominant. The strongest BVI tend to occur on the advancing side, when the axis of the tip vortex is nearly parallel to the rotor blade leading edge. Unfortunately, the accurate prediction of the unsteady airloads and resulting aeroacoustics requires predicting the location of the wake and the strength of the vortical elements to a relatively high degree of accuracy. This is beyond the scope of the present work and is an area of fervent research within the rotorcraft community.

Since the completely self-generated BVI is very complicated and difficult to accurately predict based on first principles, several simpler BVI experiments have been designed to remove some of these difficulties[16–21]. Rather than having the rotor blade interact with the self-generated wake, these experiments contain a vortex generator placed upstream of the rotor system to generate a single line vortex of known properties. The rigid rotor system is then operated at zero nominal thrust to minimize the self-generated wake. The recent experiment of Kitaplioglu and Caradonna[20,21] is extremely valuable in that acoustic measurements are available for validation. A schematic of this experiment is shown in figure 3. Unfortunately, only parallel interactions at 180 degrees of azimuth were obtained in this most recent experiment. An informal working group utilized this data to compare a wide range of methods for the prediction of BVI noise[22]. One conclusion was that simple aerodynamic methods, such as contained in the indicial approach utilizing linearized unsteady aerodynamics, were as accurate as much more expensive methods based on computational fluid dynamics (CFD) in providing

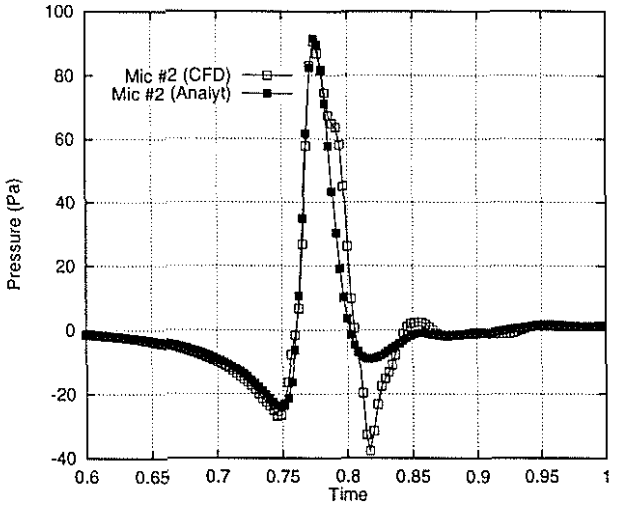

Figure 4: Comparison of acoustic signature for analytical chordwise pressure distribution and the CFD predicted chordwise pressure distribution for BVI at $M_{tip} = 0.71$ and $\mu = 0.2$.

the required airloads for subsequent linear propagation to the acoustic microphone locations. The interactions showed no sign of nonlinearities in the acoustic propagation.

As a result, in this paper, only isolated parallel interactions will be examined. After validation with experimental results and computational fluid dynamic predictions for parallel interactions occurring at 180 degrees of azimuth, more realistic parallel interactions occurring at 90 degrees of azimuth will be examined and compared to results from CFD.

Experimental/Computational Validation for Parallel Interaction at 180 Degree of Azimuth

The experimental rotor system of Caradonna and Tung, as used in the experiments of Kitaplioglu and Caradonna[20, 21] is examined to validate the linearized unsteady aerodynamics and acoustics. This rotor system consists of a two bladed untwisted rigid rectangular rotor blades of aspect ratio 7.125. In the experiment, the blades were set at zero collective to minimize self-generated BVI. The blades had a 6 inch chord with NACA 0012 airfoil section. A vortex was generated directly upstream of the rotor by an 18 inch chord, semi-span wing with a NACA 0015 airfoil section placed at an angle of attack. For this validation case of the rotor at a tip Mach number of 0.7145 and advance ratio of 0.1975, interacting with the vortex shed by the wing at an angle of attack of 12 degree passing

Microphone Number	X	Y	Z
Mic #2	-3.0	0.0	-1.87
Mic #3	-3.0	0.0	-2.26
Mic #4	-3.0	0.0	-2.80

Table 1: Coordinates of the microphones used in the experiment of Kitaplioglu and Caradonna.

one-quarter of a chord underneath the rotor blade at 180 degree of azimuth is considered for the parallel interaction case. The vortex core radius is 15% of the vortex generator chord; the nondimensional strength of the vortex is 0.36. A step size of 0.5 degree is used to rotate the blade at each time step for the indicial method while it was 0.2 degree for the CFD method. The coordinates of three of the microphone positions, using the same nomenclature to identify observer locations as in the experiment are given in Table 1. (For an interaction at 90 degree azimuth the observer locations were rotated by 90 degree such that observer locations were in front of the rotor disk).

Figure 4 shows the acoustic time signature at microphone #3 obtained using the CFD predicted chordwise pressure distribution and the analytical chordwise pressure distribution. The X-axis is time as a fraction of the time period of a rotor revolution. The comparison shows that the peak magnitude of the noise pulse obtained using the analytical pressure distribution is in excellent agreement with the noise signature obtained using the actual CFD pressure distribution. Therefore, in the rest of this paper the acoustic signature for the CFD method is obtained using the analytical chordwise pressure distribution.

The acoustic signatures are shown for microphone location #4 in figure 5 utilizing both the linearized unsteady aerodynamics from the indicial approach as well as nonlinear unsteady aerodynamics from the Euler method. Also plotted in the figure are the experimentally measured acoustic signature. It can be seen that both the peak magnitudes and the pulse width are predicted very accurately by both the CFD and the indicial method. Figure 6 shows the frequency spectra of the acoustic signature at microphone #4 for the same flight condition. Once again the indicial method is in excellent agreement with the CFD prediction over the whole range of the frequencies.

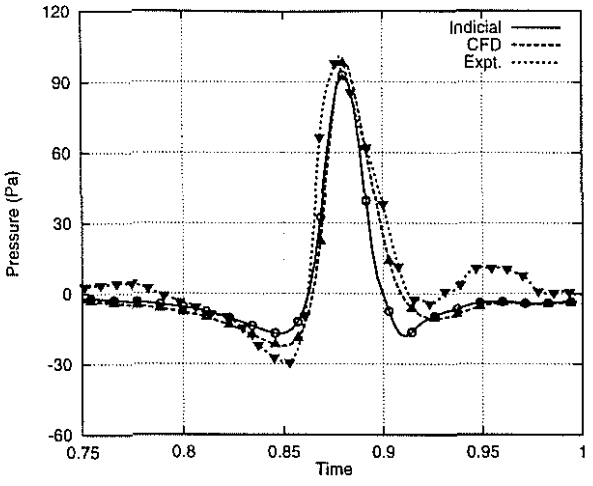

Figure 5: Comparison of acoustic signature with the experiment for BVI $M_{tip} = 0.71$ and $\mu = 0.2$.

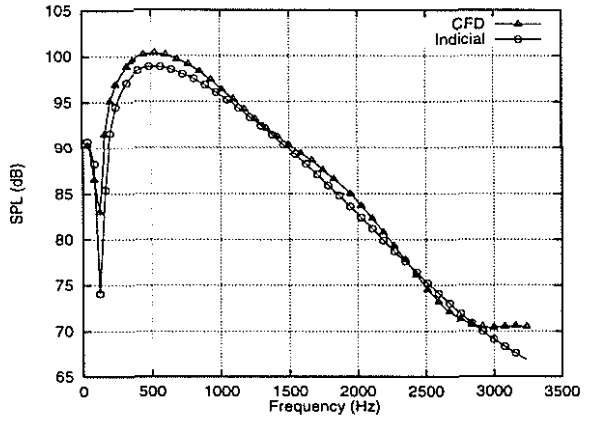

Figure 6: Frequency spectra of the acoustic signature at microphone #4 predicted using CFD and indicial method for BVI at $M_{tip} = 0.71$ and $\mu = 0.2$.

Computational Validation for Parallel Interactions at 90 Degrees of Azimuth

In this section results are presented for the aerodynamic lift time history and the resulting acoustic signature BVI computed using both the indicial method and the Euler method. In all these cases, the isolated vortex passes one-quarter of a rotor blade chord underneath the rotor blade at 90 degree of azimuth. No experimental data is available for such an interaction. For all of the results shown here 60 and 36 elements were used in the chordwise and spanwise directions respectively. Grid independence studies showed that differences in the acoustic signature were indistinguishable even if half as many points were used in either the chordwise or spanwise directions.

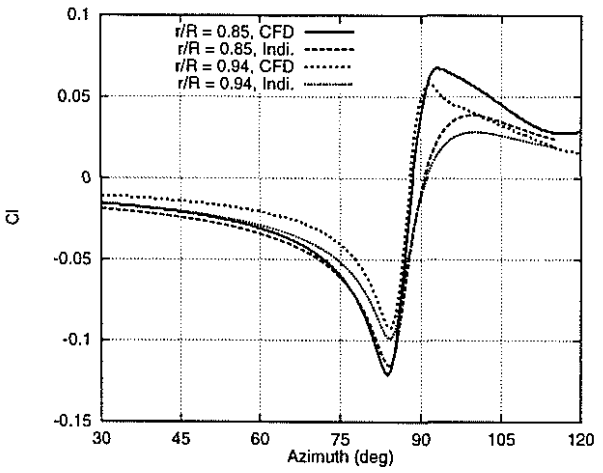

Figure 7: Unsteady lift time history for parallel BVI interaction at $\Psi = 90°$ for rotor at $M_{tip} = 0.7$ and $\mu = 0.2$

Figure 7 shows the unsteady aerodynamic loads at two outboard radial stations on the blade obtained using the indicial method (linear aerodynamics) and the Euler method (non linear aerodynamics) for an advance ratio of 0.2 and a tip Mach number of 0.7. It can be seen from this figure that even at such high advancing tip Mach numbers (0.84) the indicial method does fairly well in predicting the unsteady aerodynamic loads. The agreement is excellent before the interaction occurs. Since the interaction with the vortex results in the formation of shocks on the blade surface and therefore significant non-linearities in the aerodynamic flowfield are generated, it is not surprising that the positive loading after the interaction (at an azimuth after 90 degrees) is somewhat different. However, the large slope right after the negative loading peak is very well predicted. Even better correlation is obtained for lower advancing tip Mach numbers.

In figure 8 the acoustic time histories for parallel BVI at $M_{tip} = 0.6$ and $\mu = 0.2$ occurring on the advancing blade at 90 degree and at 180 degree are plotted for the same locations relative to the rotor in the rotor fixed frame. Results obtained using CFD are also shown to further validate the accuracy of the indicial method. It can be seen that the interaction occurring on the advancing blade results, for reasons mentioned previously, in about 30% higher peak noise amplitude for the same flight conditions.

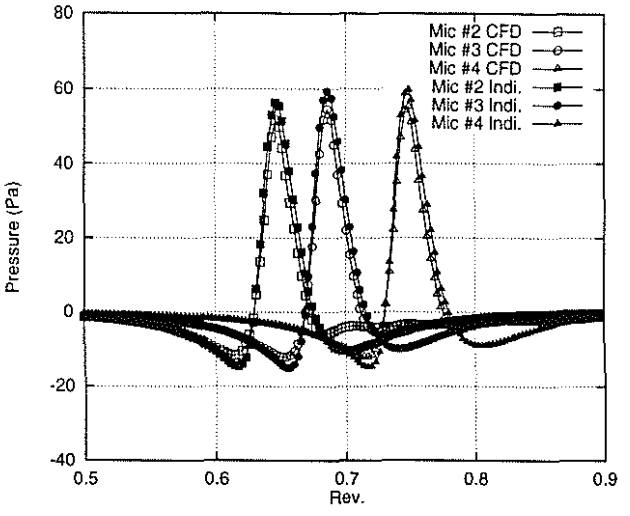

(a) $\Psi = 180°$

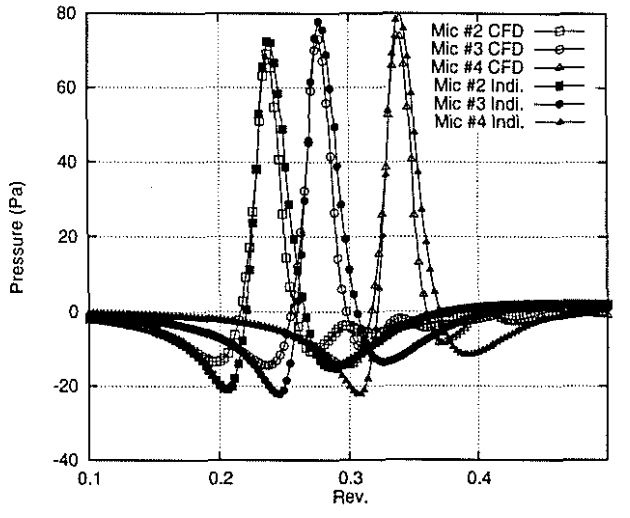

(b) $\Psi = 90°$

Figure 8: Far-field acoustic signature for parallel BVI interaction at $\Psi = 180°$ and $\Psi = 90°$ for rotor in forward flight at $M_{tip} = 0.6$ and $\mu = 0.2$.

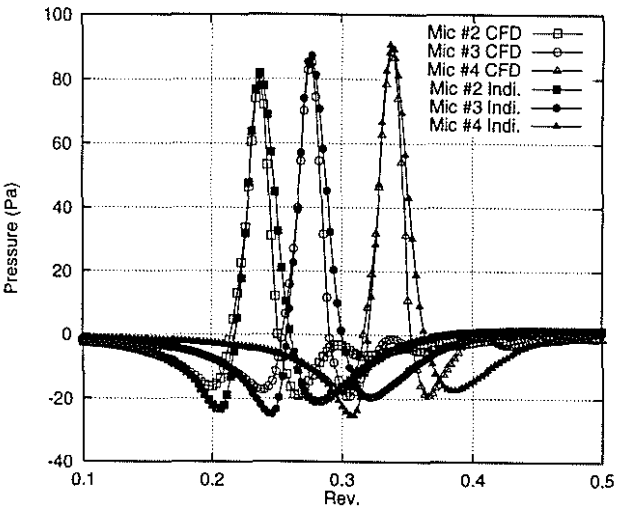

(a) $\lambda = 0.9$

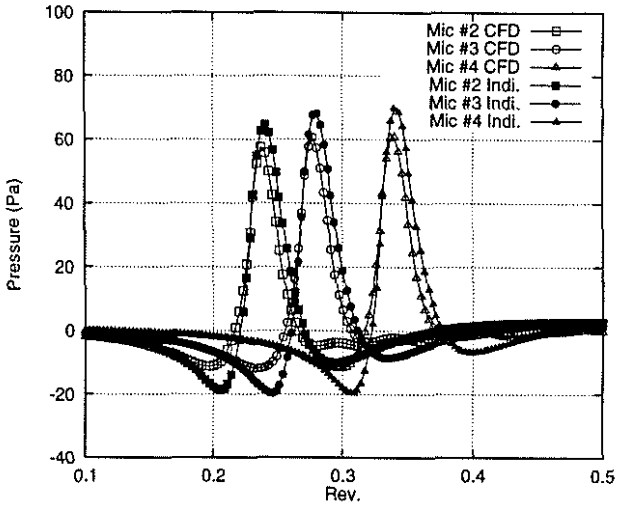

(b) $\lambda = 1.1$

Figure 9: Far-field acoustic signature for various speed ratios of the vortex convection velocity for rotor with $M_{tip} = 0.6$ and $\mu = 0.2$.

In figure 9 the acoustic signature for BVI at the same three microphone locations are plotted for an interaction with $M_{tip} = 0.60$ and $\mu = 0.2$ for two different vortex speed ratios. It can be readily observed that indicial method predicts peak amplitude accurately for all the cases. For $\lambda = 0.9$, which represents a faster moving vortex, the peak amplitudes are about 20% higher than the peak amplitude obtained for $\lambda = 1.1$.

To demonstrate the importance of including λ as a parameter in the gust response approximation, the BVI is calculated using a stationary gust function (SGF) and the general gust function (GGF). The stationary gust function is optimized for stationary gusts ($\lambda = 1$) only. This is typically the way most used by current comprehensive codes to calculate unsteady aerodyanmics. However, the effects of vortex velocity on the unsteady gust field are accurately modeled.

Figure 10 shows the lift time histories at two radial stations on the blade, obtained using GGF and SGF. For both span locations the negative peak magnitude of the lift predicted by SGF increases with λ while GGF predicts the peak magnitude to

λ	CFD	Indicial (GGF)	Indicial (SGF)
0.9	79.76	81.68	67.87
1.0	69.07	73.05	73.05
1.1	57.48	64.51	75.91

Table 2: Positive pressure peak magnitude of the acoustic pulse at Microphone #2 for BVI at $M_{tip} = 0.60$ and $\mu = 0.2$.

be almost flat. It should be noted that the Euler solver also predicts lift time histories consistent with the results obtained using GGF. With the SGF, the difference in the two lift time histories for a faster and a slower gust consists primarily of an increased magnitude of the unsteady loads for the slower moving gust, but almost no change in the maximum rate of change of lift. This is because only the effect of the changing vortex velocity is included, the aerodynamic response function remains unchanged. With the GGF, the changing aerodynamic response function is also included; resulting in the relatively minor change in the peak magnitude with gust ratio. However, it can also be noticed that the maximum rate of change of the unsteady lift is increased for the faster moving gust, relative to the slower moving gust.

Figure 11 compares the acoustic time signatures for the isolated BVI interaction using the stationary and generalized gust functions. It can be observed from the figures that if the stationary gust response is used, the noise is underpredicted for λ less than 1 while it is over predicted for the vortex moving with λ greater than 1. This is in contrast to the trend seen in figure 9 where the acoustic peak magnitude was observed to increase with the convection speed of the vortex. Table 2 shows the positive pressure peak magnitudes for the two cases along with for $\lambda = 1$. It can be concluded that a general gust function is able to predict the acoustics very close to that from the Euler solver. On the other hand, neglecting the effects of the gust motion on the response function incurs significant errors. These observations are consistent with the results for 2-D airfoil vortex interaction computations obtained using GGF and SGF[5].

Conclusion

The far-field noise of an isolated parallel BVI on an advancing rotor blade is calculated using the indicial method with a general gust function. It is shown that such an indicial method can be used

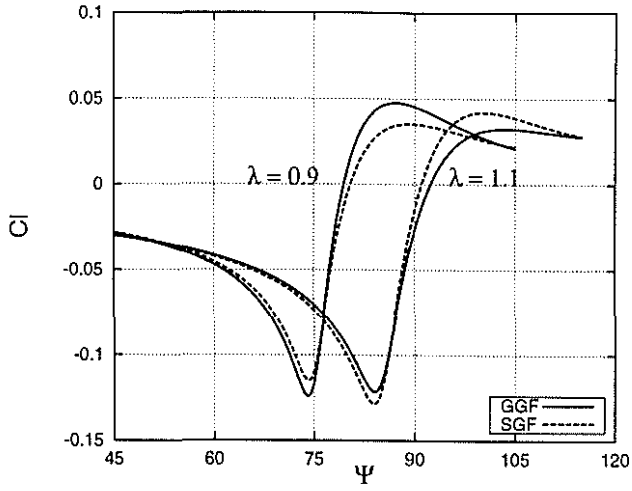

(a) r/R = 0.94

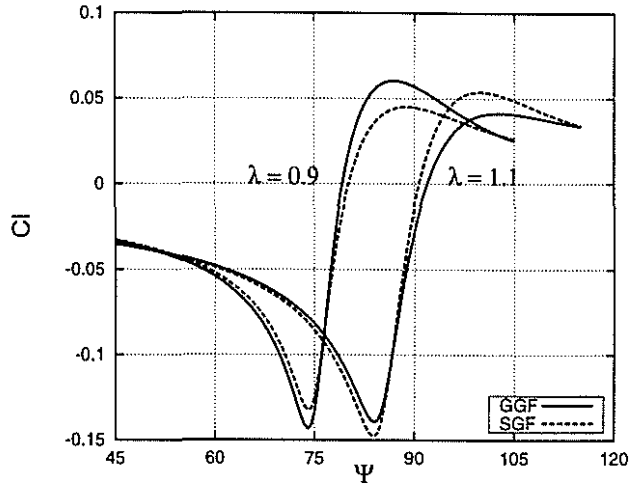

(b) r/R = 0.85

Figure 10: Aerodynamic load time history at two span locations obtained using general gust function (GGF) and stationary gust function (SGF) for BVI at $M_{tip} = 0.60$ and $\mu = 0.2$.

to accurately calculate the unsteady aerodynamic loads and the resulting acoustics of BVI. It is also shown that the vortex convection speed has a significant influence on the peak amplitude of the far-field noise and use of general gust function allows the indicial method to capture this effect accurately. For the specific case presented, an approximately 20% decrease in the gust ratio resulted in a 20% increase in the maximum peak pressure in the far-field. This is consistent with results from an Euler solver. However, failure to properly model the aerodynamic response, by using the stationary

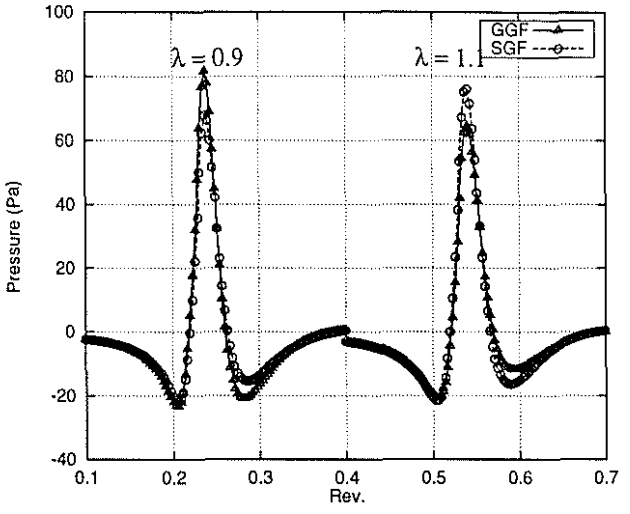

(a) Mic # 2

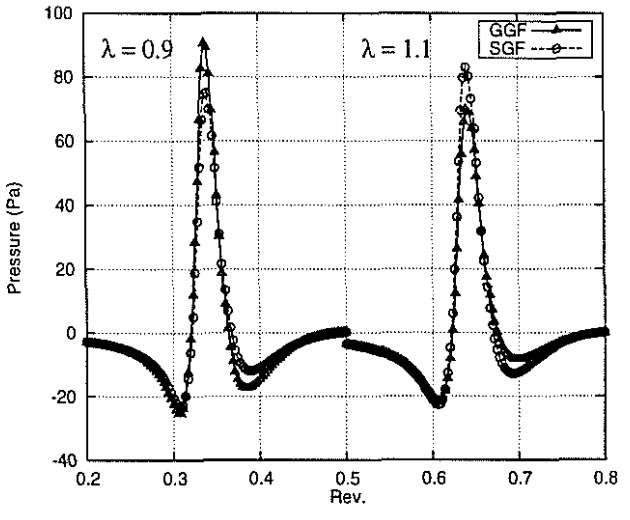

(b) Mic # 4

Figure 11: Acoustic signature obtained using general gust function (GGF) and stationary gust function (SGF) for BVI at $M_{tip} = 0.60$ and $\mu = 0.2$.

gust function, results in the incorrect trend. Therefore, it is recommended that comprehensive codes be modified to include generalized gust functions.

References

[1] Lomax, H., "Indicial Aerodynamics," Chapter 6, AGARD Manuel on Aeroelasticity, October 1968.

[2] Tobak, M., and Schiff, L.B., "Aerodynamic Mathematical Modeling - Basic Concepts," Dynamics Stability Parameters, *AGARD LS-114*, 1981.

[3] Beddoes, T.S., "Practical Computation of Unsteady Lift," *Vertica*, Vol. 8, No. 1, 1984, pp.55-71.

[4] Leishman, J.G., " Modeling of Subsonic Unsteady Aerodynamics for Rotary Wing Applications," *Journal of the American Helicopter Society*, Vol. 35, No. 1, Jan. 1990, pp.29-38.

[5] Singh, R., and Baeder, J.D., "Generalized Moving Gust Response Using CFD with Application to Airfoil-Vortex Interaction" *15th AIAA Applied Aerodynamics Conference, Atlanta*, June 1997.

[6] Leishman, J.G., "Unsteady Aerodynamics of Airfoils Encountering Traveling Gusts and Vortices," *to appear in Journal of Aircraft*

[7] Leishman, J.G., "Subsonic Unsteady Aerodynamics Caused by Gusts Using the Indicial Method", *Journal of Aircraft*, Vol. 33, No. 5, Sept-Oct 1996.

[8] Srinivasan, G.R. and Baeder, J.D., "TURNS: A Free Wake Euler/ Navier-Stokes Numerical Method for Helicopter Rotors," *AIAA Journal*, Vol.31 No. 5, May 1993.

[9] Baeder, J.D., and Srinivasan, G.R., "Computational Aeroacoustics Study of Isolated Blade-Vortex Interaction Noise", Presented at the American Helicopter Society Aeromechanics Specialists Conference, San Francisco, CA, Jan. 1994.

[10] Baeder, J.D., "Passive Design for Isolated Blade-Vortex Interaction Noise Reduction", *53rd American Helicopter Society Forum*, Virginia Beach, VA, 1997.

[11] Srinivasan, McCroskey, W.J., and Baeder, J.D., "Aerodynamics of Two-Dimensional Blade-Vortex Interaction," *AIAA Journal*, Vol. 24, No. 10, October 1986.

[12] Parameswaran, V., and Baeder, J.D., "Indicial Aerodynamics in Compressible Flows - Direct Computational Fluid Dynamic Calculation," *Journal of Aircraft*, Vol 34, No.1, Jan-Feb 1997.

[13] Brentner, K.S., "Prediction of Helicopter Rotor Noise - A Computer Program Incorporating Realistic Blade Motions and Advanced Formulation", *NASA TM 87721*, 1986.

[14] Lighthill, M.J., "On Sound Generated Aerodynamically", *Philosophical Transactions of the Royal Society*, A564, 1952.

[15] Ffowcs Williams, J.E., and Hawkins, D.L., " Sound Generated by Turbulence and Surfaces in Arbitrary Motion", *Philosophical Transactions of the Royal Society*, A264, 1969.

[16] Surendriah, M., "An Experimental Study of Rotor Blade-Vortex Interaction," *NASA CR-1753*, May 1970.

[17] Caradonna, F. X., Laub, G. H., and Tung, C., "An Experimental Investigation of the Parallel Blade-Vortex Interaction," *Workshop on Blade Vortex Interaction, NASA Ames Research Center*, Oct. 1984.

[18] Kokkalis, T., and Galbraith, R. A., "Description of, and Preliminary Results from a New Blade-Vortex Interaction Test Facility," *12th European Rotorcraft Forum*, Garmish, Germany, Sept. 1986.

[19] Seath, D. D., Kim, J. M., and Wilson, D. R., "An Investigation of the Parallel Blade-Vortex Interaction in a Low Speed Wind-Tunnel," *AIAA Paper 87-1344, 19th Fluid Dynamics*, Plasma Dynamics and Lasers Conference, Honolulu, HA, June, 1987.

[20] Kitaplioglu, C., Caradonna, F.X., " Aerodynamics and Acoustics of Blade-Vortex Interaction Using an Independently Generated Vortex," *American Helicopter Society Aeromechanics Specialists Meeting*, San Francisco, Jan. 1994.

[21] Kitaplioglu, C. and Caradonna, F. X., "Parallel Blade-Vortex Interactions: An Experimental Study and Comparison with Computation," *American Helicopter Society Aeromechanics Specialists Conference*, Bridgeport, CT, Oct., 1995.

[22] Caradonna, F.X., et al., " A Review of Methods for the Prediction of BVI Noise," *American Helicopter Society technical Specialists Meeting for Rotorcraft Acoustics and Aerodynamics,* Williamsburg, VA., Oct., 1997.